Supplement of: PM$_1$ composition and source apportionment at two sites in Delhi, India across multiple seasons

S1. Monitoring sites, meteorology and dates.
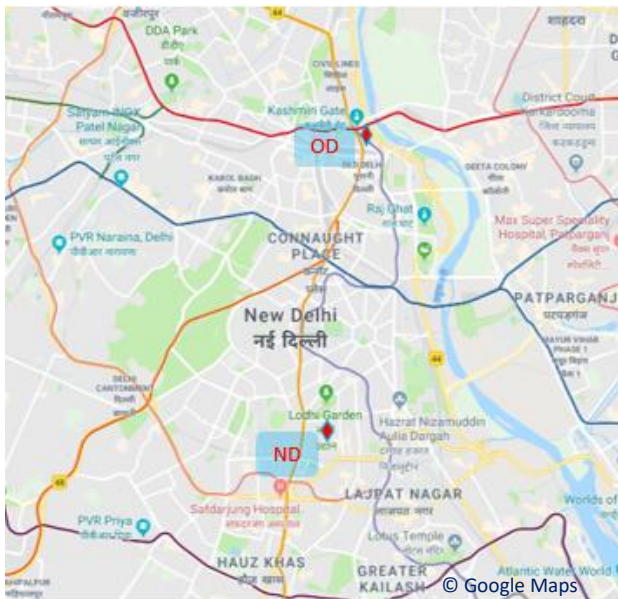
Figure S1 Location of the monitoring sites. Image taken from www.googlemaps.co.uk IGDTUW located at Old Delhi Lat 28.588°, Lon 77.217° and IMD located at New Delhi Lat 28.664°, Lon 77.232°.
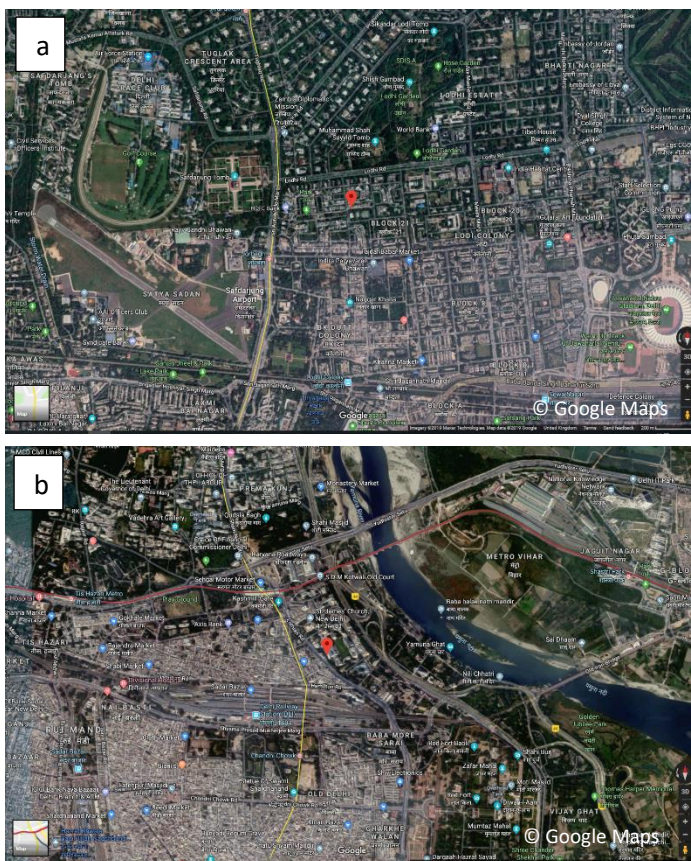
Figure S2 Maps showing the surroundings of ND (a) and OD (b). Red circle shows location of the monitoring sites.
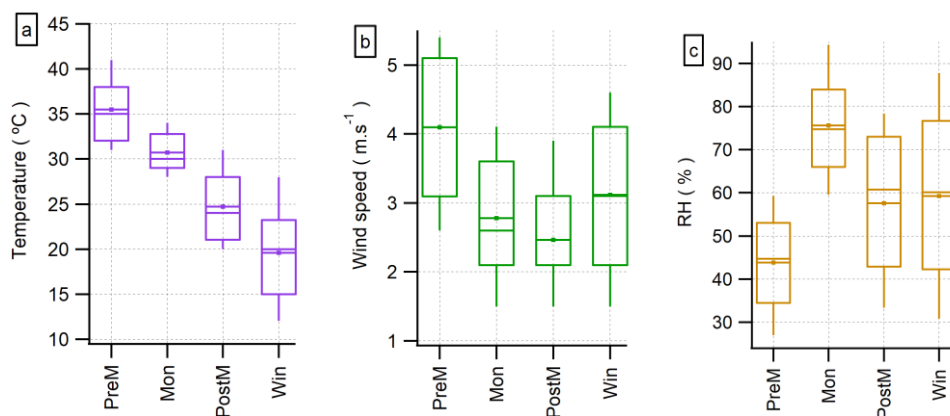
Figure S3 Box plots with temperature (a), wind speed (b) and relative humidity (c) for the different seasons. The marker represents the mean.

Table S1 Collocated instruments with the mass spectrometers.

Instrument	Event	Aditional instrumentation
ACSM	Win_ND_A	Aethalometer AE33
HR-AMS_1	PreM_ND_H1	Aethalometer AE31
cToF-AMS	PreM_OD_C	Aethalometer AE31
HR-AMS_2	PreM_OD_H2	Aethalometer AE31
HR-AMS_2	Mon_OD_H2	Aethalometer AE31
HR-AMS_2	PostM_OD_H2	Aethalometer AE31, SP2, PTR-MS, Nox, CO
cToF-AMS	PostM_OD_C	Aethalometer AE31
HR-AMS_2	PostM_OD_T_H2	Aethalometer AE31
cToF-AMS	PostM_ND_T_C	MAAP

S2. AMS quality assurance analysis. NR-PM$_1$ concentrations and relative contribution

S2.1 Calibrations and collection efficiency estimation.

Table S2. Nitrate ion efficiency (IE) and relative IE (RIE) for NH4$^+$, SO4^{2-} and Cl$^-$ from calibrations performed to the aerosol mass spectrometer instruments.

Instrument	Season	IE	RIE_NH$_4^+$	RIE_SO$_4^{2-}$	RIE_Cl$^-$	CE
cToF-AMS	PreM	1.55E-07	4.01	1.17	1.5	0.5
cToF-AMS	PostM	2.40E-07	4.6	1.2	1.7	0.5
HR-AMS_1	PreM	3.25E-08	4	1.31	1.3	0.5

The collection efficiency (CE) applied to the instruments was 0.5. This value was selected after comparing the HR-AMS_2 with filter measurements (Fig. S4). Also, the ACSM manual recommends to use a CE = 0.5.
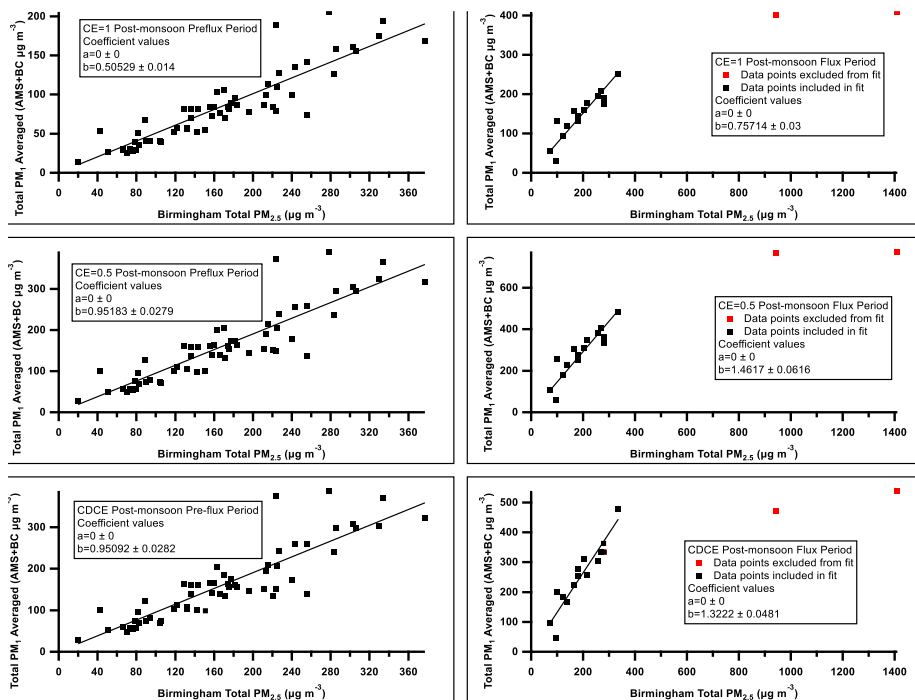
Figure S4 Comparison of total PM1 with filter measurements to determine collection efficiency (CE) with HR-AMS_2 and aethalometer (BC) measurements.

S2.1 cToF-AMS and HR-AMS_2 intercomparison.

An intercomparison was performed between the cToF-AMS and the HR-ToF-AMS, deployed at OD over pre-monsoon in order to perform an intercomparison (28/May – 09/June), obtaining average concentrations of 15.0 and 19.1 of Org, 1.7 and 1.6 of NO_3^-, 6.8 and 8.3 of SO_4^{2-}, 2.5 and 2.6 of NH_4^+, 0.4 and 0.5 of Cl^-. for cToF and HR-ToF respectively.
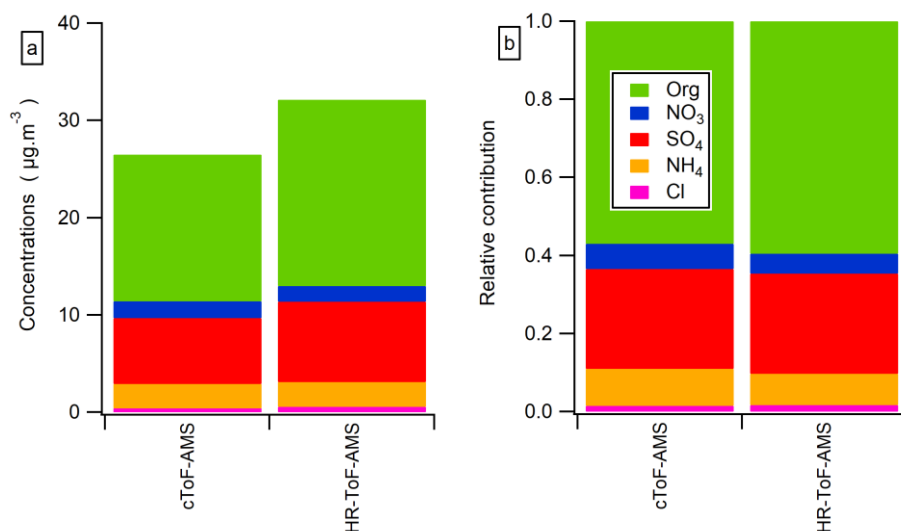
Figure S5. Average concentrations (4.a) and relative contribution (4.b) of Org, NO₃, SO₄, NH₄ and Cl for the different events. Mon = Monsoon. T = Tower measurements.

Table S3. Statistics of NR-PM1 and BC measurements for the various seasons. Minimum, maximum, average, standard deviation, median and number of points.

	Org						no3						so4					
	min	max	avg	SD	median	npnts	min	max	avg	SD	median	npnts	min	max	avg	SD	median	npnts
Win_ND_A	5.27	197.60	39.88	32.22	29.98	2169	0.18	21.05	3.69	2.96	2.82	2169	0.84	9.77	3.90	1.82	3.66	2169
PreM_ND_H1	-0.67	788.67	23.59	21.76	19.58	40569	-0.05	16.44	2.33	2.21	1.55	40569	-0.11	21.57	5.03	3.24	4.10	40569
PreM_OD_C	3.01	283.67	30.20	26.21	24.10	3196	0.42	15.27	3.41	2.59	2.48	3196	0.24	30.12	13.54	5.11	12.39	3196
PreM_OD_H2	-0.05	291.76	29.16	22.96	26.12	11808	0.02	16.28	2.31	2.39	1.50	11808	0.00	43.17	13.05	6.39	12.71	11808
Mon_OD_H2	-0.11	195.86	24.98	16.63	21.43	4384	0.02	22.88	3.14	2.66	2.41	4384	-0.01	37.77	11.29	5.56	9.90	4384
PostM_OD_H2	9.02	458.35	95.35	68.11	75.06	6798	1.65	58.66	11.45	8.15	9.25	6798	2.14	30.09	11.01	5.33	10.24	6798
PostM_OD_C	13.19	206.78	62.97	39.39	55.12	1044	0.72	35.73	7.69	6.80	5.24	1044	1.71	25.19	8.82	3.54	8.77	1044
PostM_OD_T_H2	10.37	1211.58	87.85	77.59	75.98	1785	1.79	28.09	12.02	5.19	12.20	1785	0.55	52.66	6.77	4.61	6.22	1785
PostM_ND_T_C	13.93	331.73	73.23	42.31	62.77	1506	1.56	42.72	14.44	8.23	13.51	1506	-1.76	35.49	6.58	3.13	6.55	1506
	nh4						chl						BC					
	min	max	avg	SD	median	npnts	min	max	avg	SD	median	npnts	min	max	avg	SD	median	npnts
Win_ND_A	-2.40	28.74	4.54	4.11	3.07	2169	-0.10	67.59	5.96	9.14	2.35	2169	1.064	77.02	15.91	13.62	10.69	2144
PreM_ND_H1	-1.50	16.58	2.63	1.78	2.18	40568	-0.30	26.57	1.15	1.75	0.54	40569	0.354	8.929	2.529	1.46	2.324	529
PreM_OD_C	-6.19	13.66	5.02	1.90	4.63	3196	0.03	22.73	0.80	1.78	0.26	3196	0.027	51.53	5.918	4.731	4.646	2684
PreM_OD_H2	-0.01	20.79	4.16	2.35	3.90	11808	0.00	33.75	1.29	2.57	0.44	11808	0.027	51.53	5.895	5.367	4.435	6688
Mon_OD_H2	0.00	18.23	3.75	2.04	3.39	4384	0.00	34.30	0.99	1.66	0.37	4384	0.076	20.02	3.936	2.642	3.208	4314
PostM_OD_H2	0.66	37.60	7.47	5.31	6.06	6798	0.07	59.96	6.05	7.48	2.91	6798	0.608	53.76	11.59	10.01	8.08	5499
PostM_OD_C	-8.22	15.18	5.02	3.19	4.22	1044	0.07	28.69	3.91	5.00	2.08	1044	1.114	31.76	7.783	5.563	6.93	914
PostM_OD_T_H2	0.55	44.50	8.75	5.16	8.69	1785	0.30	73.80	9.67	10.91	5.43	1785	1.585	59.52	17.27	13.56	12.24	1497
PostM_ND_T_C	-5.54	28.43	7.41	4.04	7.09	1506	0.15	56.52	5.03	5.66	3.07	1506	3.316	38.17	16.52	7.708	16.03	1103
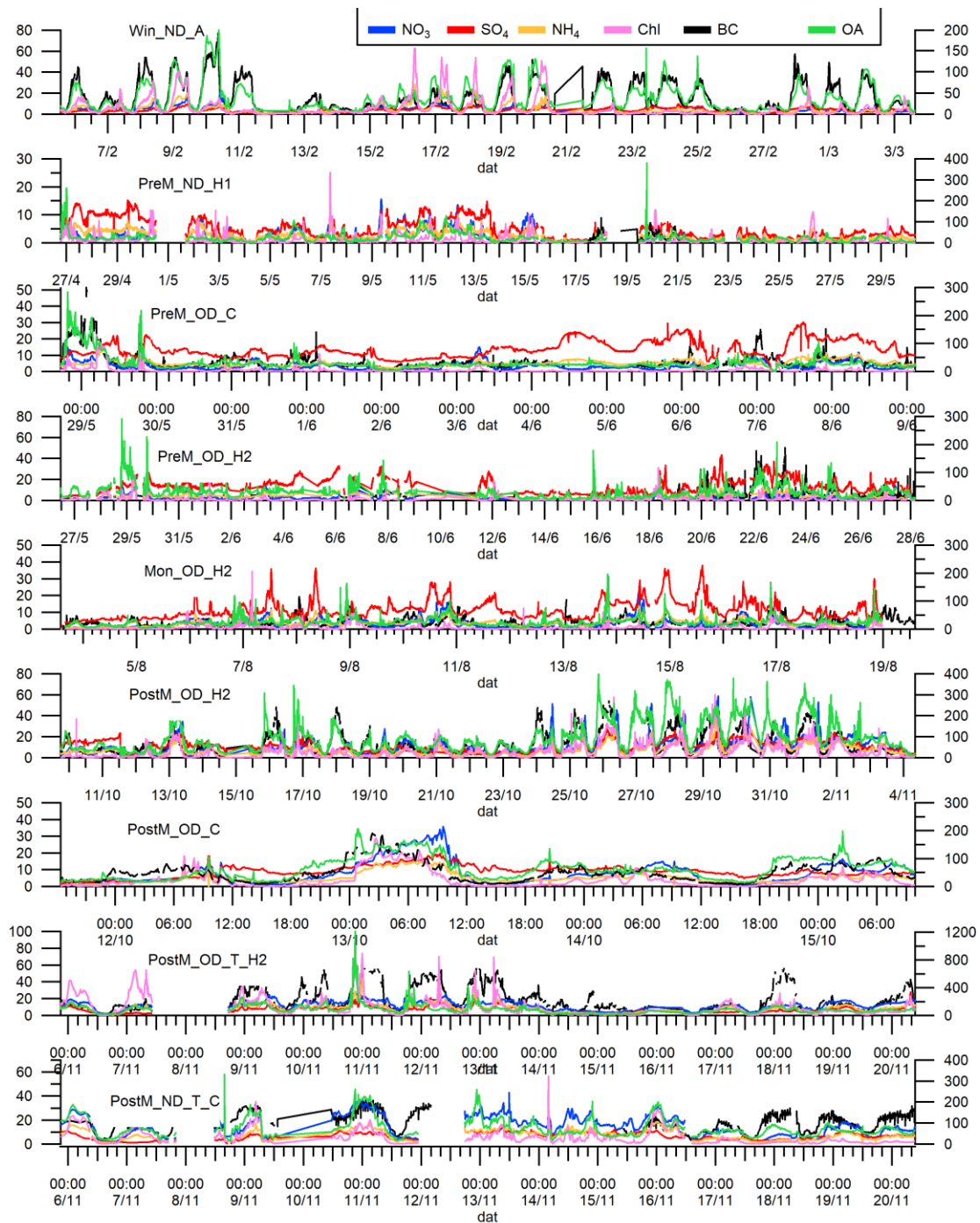
Figure S6. Aerosol time series of the various measurements. All concentrations are in µg.m^{-3}. OA concentrations are plotted on the right axis and the rest of the compounds are plotted on the left axis.

S3. PMF analysis

The selection of the optimal PMF solution was performed following recommendations in previous studies (Canonaco et al., 2013;Crippa et al., 2014;Reyes-Villegas et al., 2016) and exploring between 8-10 PMF solutions with 3, 4, 5 and 6 factors; looking at different seeds (a random starting point of the PMF solution), which resulted on analysing around 40 PMF solutions per season.

The following criteria was used to select the optimal PMF solution:

1. Residuals to be closest to zero.
2. Q/Q_{exp} value closest to one.
3. High correlation between HOA and NOx.

In all the PMF analyses, an improvement in the residuals and Q/Q_{exp} was observed when increasing the number of factors (Fig. S6). However, the 6-factor solutions presented two factors with similar time series and mass spectra, characteristic of factor splitting. Hence, the 5 factor solution was chosen to be further analysed.

The following figures show the PMF solution space to select the optimal PMF solution for the winter New Delhi ACSM dataset, Win_ND_A. The same analysis was performed to the other datasets to determine the optimal PMF solution for each season for further analysis presented in the manuscript.

The solutions are labelled as follows: PMF_4F_S1 is the 4-factor solution (4F) seed number one (S1). The optimal solution of this season is PMF_5F_S2. This solution showed the lowest average residuals and Q/Qexp value (Figure S6). Detailed residuals and Q/Qexp values for time series (Fig. S7) and m/z (Fig. S8) are also presented. In figure S9 the Pearson values from linear regressions between the PMF factors and NOx are displayed. NOx is a pollutant well-known to be related to traffic emissions, thus a high Pearson value is expected between HOA and NOx. High pearson values between 0.77 – 0.785 were observed with the highest Pearson value to be found with the PMF_5F_S2 solution (0.785).
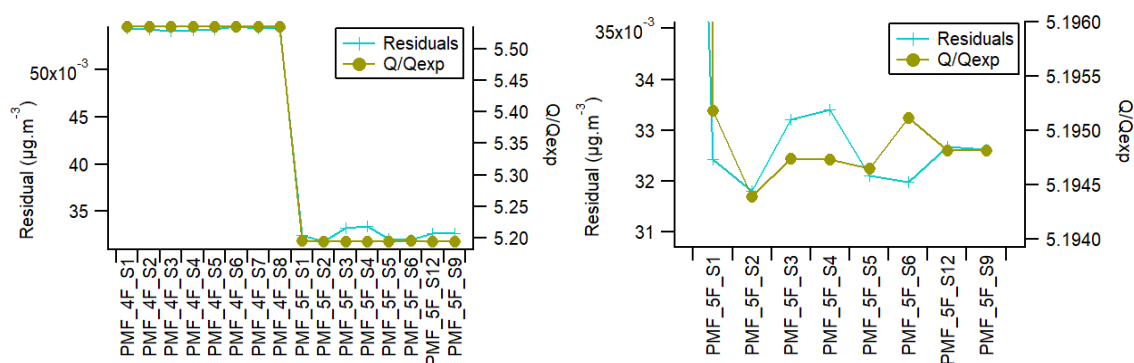
Figure S7. Summary plots of residuals and Q/Qexp values for 4 and 5 factor solutions (a) and a close up to the 5-factor solutions (b)
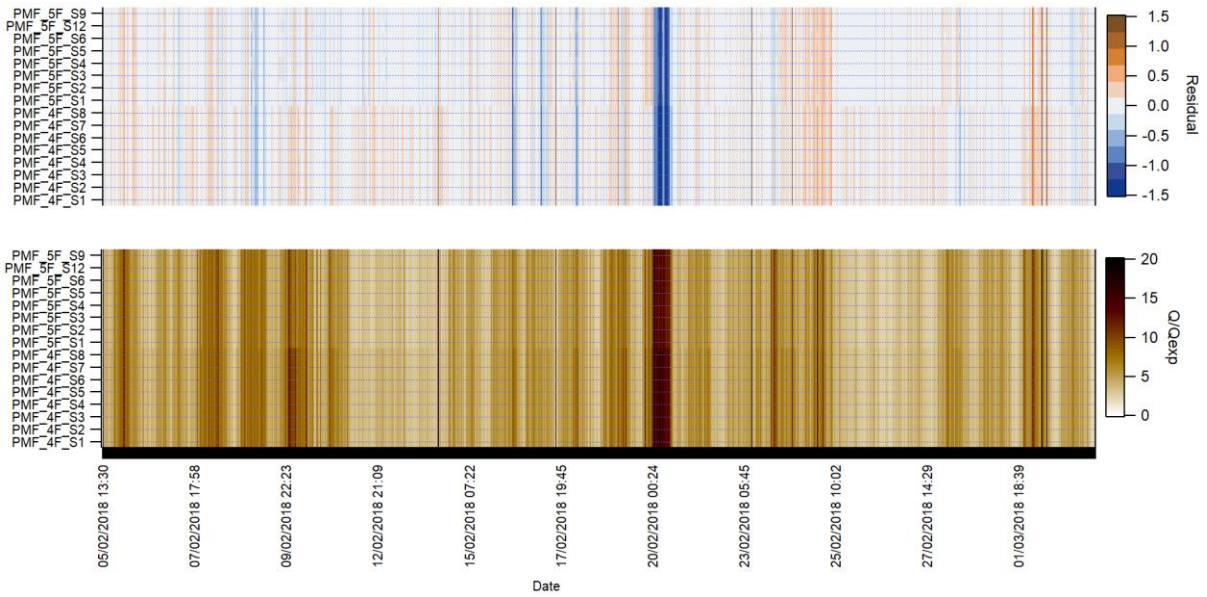
Figure S8. Time series of residuals and Q/Qexp values.
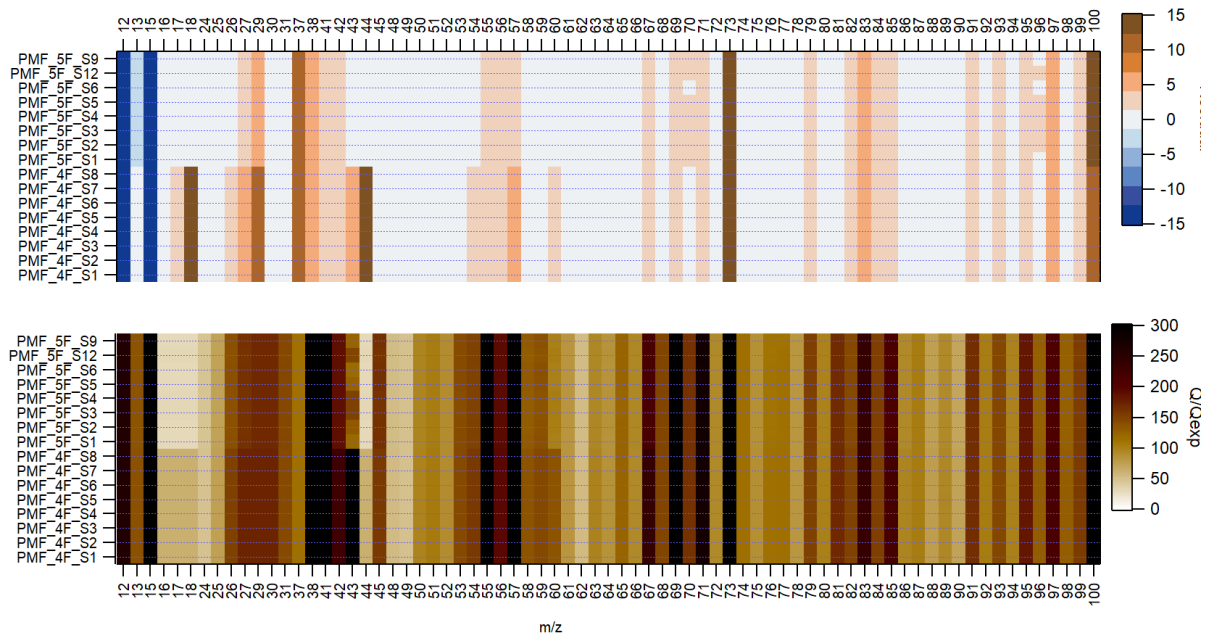
Figure S9. Residuals and Q/Qexp values fo the m/z.
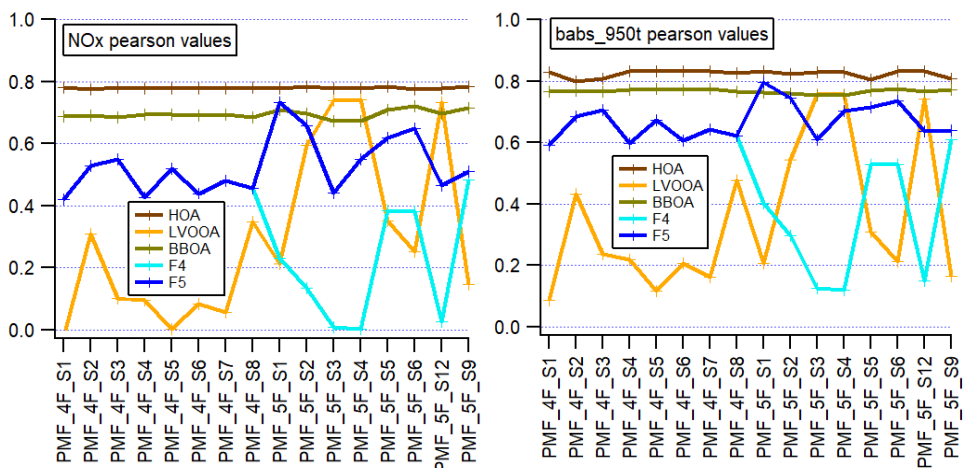
Figure S10. Pearson values of the linear regressions between the PMF factors and NOx (a) and babs_950t (b).

Table S4. Statistical parameters [μg.m^{-3}] of the PMF factors obtained from OA, measured with the HR- AMS_2, for all the various seasons. This data is analysed on detail by Cash et al. (2020), we present this data here to compare with the other PMF-AMS datasets.

	COA	HOA_	LVOOA	NHOA	SFOA	SVBBOA	SVOOA	HOA	BBOA	POA	SOA	TOA	POA ratio
All_OD_H2 (includes PreM, Mon and PostM)													
mean	7.44	9.35	13.72	4.87	6.64	7.03	5.36	14.21	13.67	35.32	19.08	54.40	0.55
median	5.26	4.31	12.14	0.30	0.74	0.04	4.00	4.88	1.80	14.74	17.81	32.83	0.55
sd	9.55	14.30	10.89	12.65	16.05	12.81	5.85	25.71	26.45	51.35	13.21	58.69	0.21
min	0.00	0.00	0.00	0.00	0.00	0.00	0.00	0.00	0.00	0.00	0.00	0.00	0.00
max	202.87	189.56	90.90	337.90	665.03	91.39	66.84	337.90	709.60	1250.37	103.93	1250.37	1.00
PreM_OD_H2													
mean	7.84	5.13	10.59	0.83	1.16	0.53	3.26	5.96	1.68	15.48	13.85	29.33	0.52
median	5.61	3.07	10.68	0.00	0.07	0.00	1.57	3.25	0.43	10.15	14.18	26.44	0.50
sd	8.73	6.90	7.36	2.46	3.51	1.18	4.76	8.80	3.91	17.95	9.70	23.54	0.22
min	0.00	0.00	0.00	0.00	0.00	0.00	0.00	0.00	0.00	0.00	0.00	0.00	0.00
max	131.02	118.38	53.01	30.06	75.91	12.97	56.72	136.58	84.70	233.64	61.50	290.36	1.00
Mon_OD_H2													
mean	2.83	6.55	6.71	0.76	1.36	0.01	6.81	7.31	1.37	11.51	13.52	25.03	0.45
median	1.79	4.84	6.32	0.19	0.50	0.00	5.41	5.18	0.51	8.58	12.90	21.35	0.43
sd	3.57	5.62	5.11	1.33	3.33	0.11	5.80	6.68	3.34	11.09	8.37	16.77	0.19
min	0.00	0.00	0.00	0.00	0.00	0.00	0.00	0.00	0.00	0.00	0.00	0.00	0.01
max	41.95	59.34	35.68	14.61	60.78	3.07	66.84	67.70	60.78	130.85	66.84	197.70	1.00
PostM_OD_H2													
mean	8.54	17.78	20.56	12.95	14.90	16.85	6.97	30.73	31.75	71.02	27.53	98.55	0.63
median	6.70	8.67	19.34	4.47	7.98	11.98	5.77	13.20	21.52	48.61	25.28	77.06	0.64
sd	7.72	21.96	11.51	17.97	18.49	15.35	5.83	39.27	30.56	64.55	13.07	69.33	0.17
min	0.00	0.00	0.00	0.00	0.00	0.00	0.00	0.00	0.00	3.25	0.00	9.05	0.24
max	101.75	189.56	90.90	119.01	186.96	91.39	44.53	281.55	247.80	456.41	103.93	460.48	1.00
PostM_OD_T_H2													
mean	9.56	11.21	24.39	9.26	21.35	26.87	8.65	20.46	48.22	78.25	33.04	111.29	0.64
median	7.22	6.51	21.51	2.93	11.05	25.44	7.89	10.19	37.41	61.87	30.82	96.55	0.63
sd	15.55	13.09	14.51	21.27	36.38	13.00	5.53	28.83	44.79	80.12	14.63	81.24	0.14
min	0.00	0.00	0.00	0.00	0.00	1.76	0.00	0.00	2.72	5.57	0.00	14.65	0.38
max	202.87	86.99	63.69	337.90	665.03	76.43	29.20	337.90	709.60	1250.37	70.89	1250.37	1.00

POA = primary OA, SOA = secondary OA, TOA = SOA +POA. This analysis identified 7 PMF factors, we are adding HOA = HOA_ + NHOA and BBOA = SFOA + SVBBOA to compare with our 5-factor solutions in the main manuscript.

S4. Aethalometer analysis

S4.1 Aethalometer AE-31 correction and model OD

The data collected with the aethalometer model AE-31 needs to be corrected from loading and scattering effects. The Weingarten model (Weingartner et al., 2003) has been applied using a filter loading factor f=1.30 and a multiple scattering constant C=2.8, which was calculated as the slope between BC from SP2 measurements and BC from Aethalometer after filter loading corrections. Figure S5 shows the corrected BC concentrations from the Aethalometer (red) and the BC concentrations of the SP2.
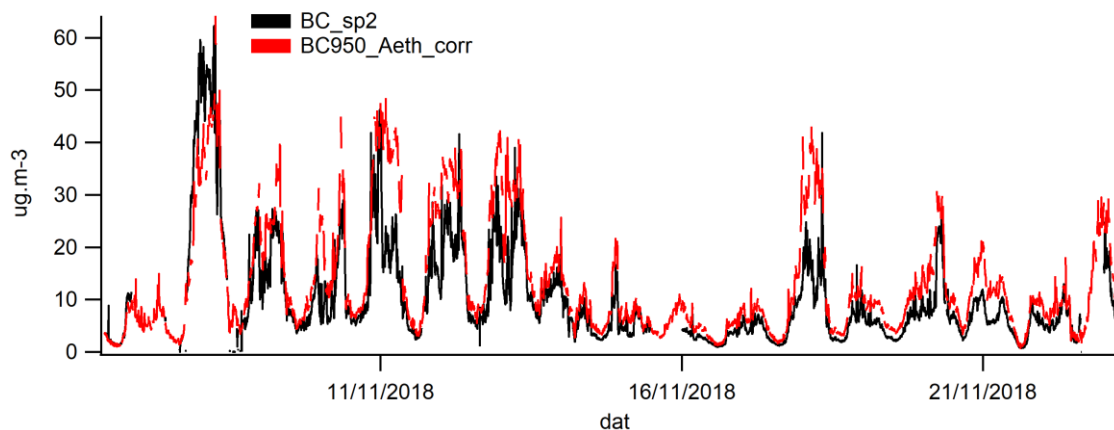
Figure S11. Intercomparison of BC measurements between aethalometer AE-31 and SP2

The aethalometer model was applied following the Sandradewi approach (Sandradewi et al., 2008) using absorption angstrom exponent traffic $\alpha_{tr} = 0.8$ and wood burning $\alpha_{wb} = 2.0$ (Fig. S6).
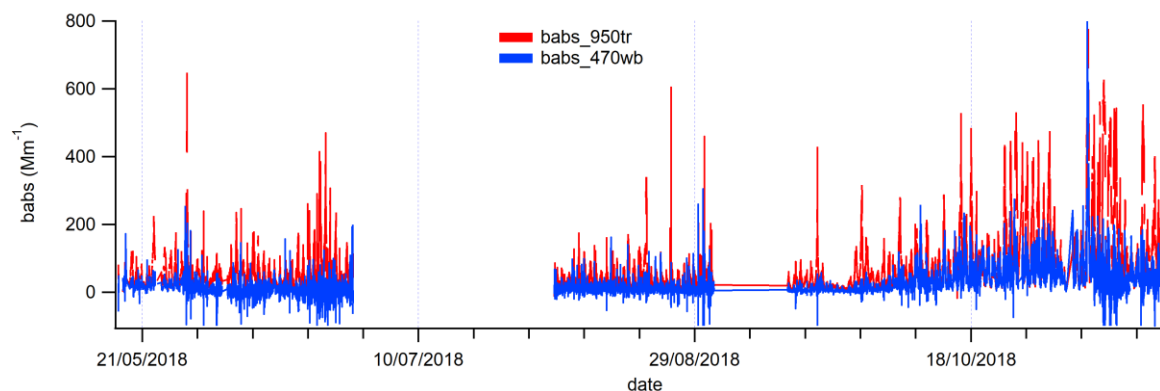
Figure S12. Aethalometer model absorption coefficients for traffic (babs_950tr) and wood burning (babs_470wb).

A sensitivity test was performed to determine $\alpha_{tr} = 0.8$. and $\alpha_{wb} = 2.0$. No significant changes were observe when testing different α_{wb} values, thus the default value of 2.0 was used (Fig. S9).
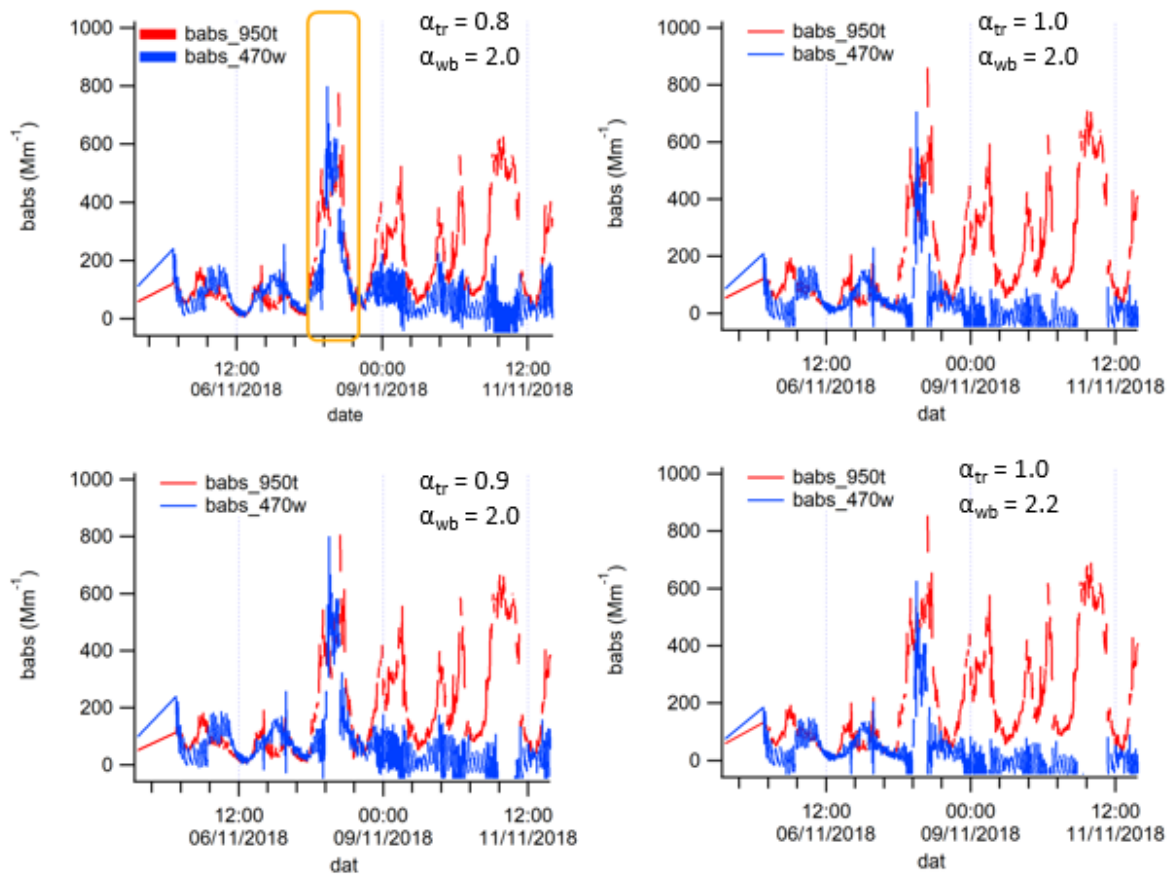
Figure S13. Sensitivity test to select α_{tr} = 0.8. The peak marked in panel (a) relates to the Diwali celebrations.

S4.2   Aethalometer model outputs AE-31 PreM_ND.

The aethalometer model was applied following the Sandradewi approach (Sandradewi et al., 2008) using an absorption angstrom exponent for traffic of α_{tr} = 0.8 and for wood burning of α_{wb} = 2.0 (Fig. S6).
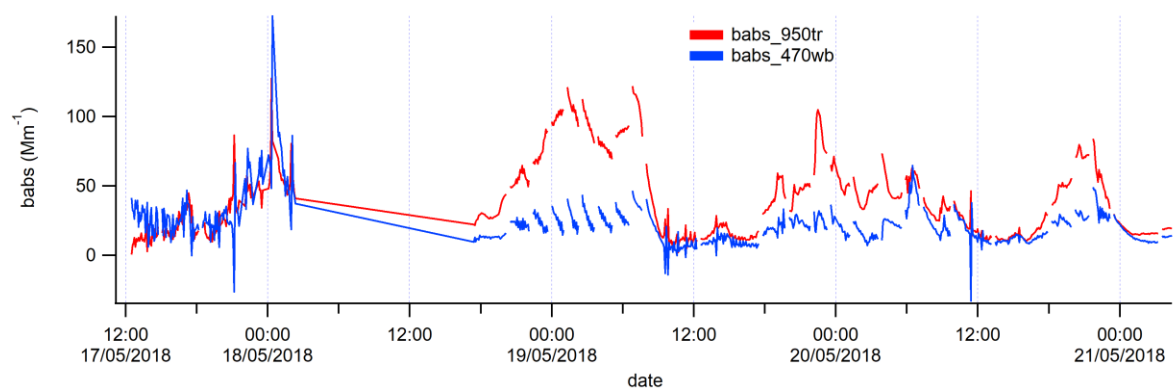
Figure S14. Aethalometer model absorption coefficients for traffic (babs_950tr) and wood burning (babs_470wb).

S4.3 Aethalometer model outputs AE-33 ND-Winter.

The aethalometer model was applied following the Sandradewi approach (Sandradewi et al., 2008) using absorption angstrom exponent traffic $\alpha_{tr} = 1.0$ and wood burning $\alpha_{wb} = 2.0$ (Fig. S8).
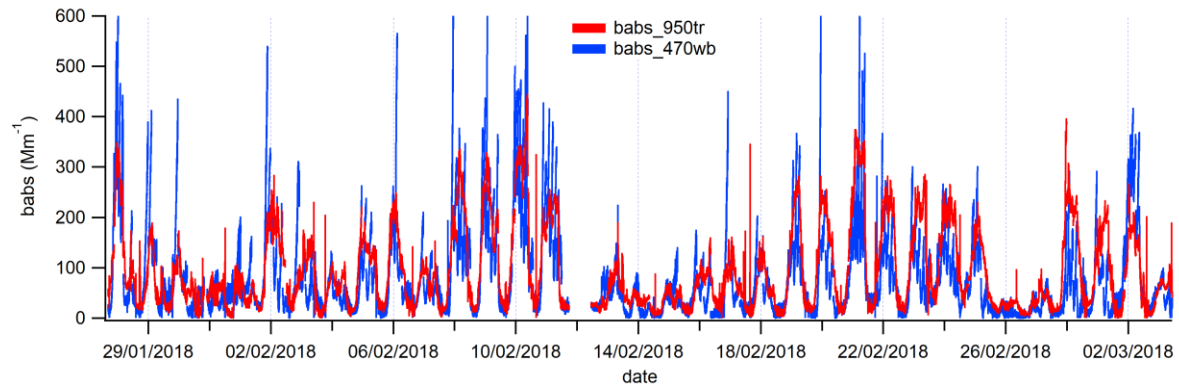
Figure S15. Aethalometer model applied to AE-33 model in Winter.

S5. Analysis of wind speed and direction.
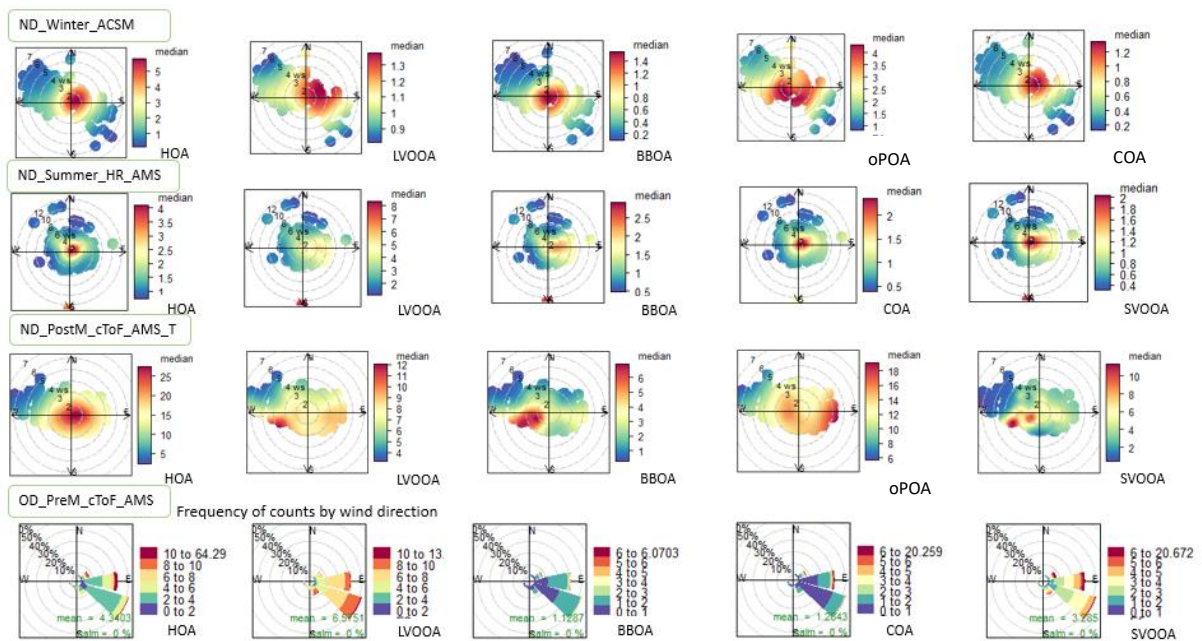
Figure S16. Polar plots of OA factors median concentrations [$\mu g.m^{-3}$]. Due to the low number of data points for OD_PreM_cToF_AMS to plot polar plots, pollution roses are presented.
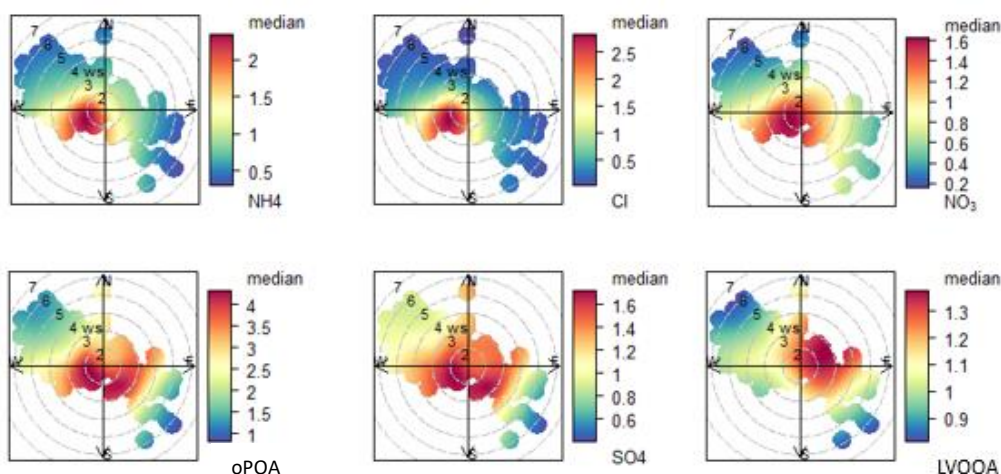
Figure S17. Polar plots of oPOA and Cl median concentrations [µg.m^{-3}].

References

Canonaco, F., Crippa, M., Slowik, J. G., Baltensperger, U., and Prevot, A. S. H.: SoFi, an IGOR-based interface for the efficient use of the generalized multilinear engine (ME-2) for the source apportionment: ME-2 application to aerosol mass spectrometer data, Atmos Meas Tech, 6, 3649-3661, DOI 10.5194/amt-6-3649-2013, 2013.

Cash, M. J., Langford, B., Di Marco, C., Mullinger, N., Allan, J., Reyes-Villegas, E., Ruthambara, J., Heal, M., Acton, W., F. J., Drysdale, W., Tuhin, M., Shivani, Ranu, G., and Nemitz, E.: High-resolution chemical characterisation of sub-micron aerosol and its seasonal contributions from sources of burning, cooking and transport in Old Delhi, In-preparation, 2020.

Crippa, M., Canonaco, F., Lanz, V. A., Aijala, M., Allan, J. D., Carbone, S., Capes, G., Ceburnis, D., Dall'Osto, M., Day, D. A., DeCarlo, P. F., Ehn, M., Eriksson, A., Freney, E., Ruiz, L. H., Hillamo, R., Jimenez, J. L., Junninen, H., Kiendler-Scharr, A., Kortelainen, A. M., Kulmala, M., Laaksonen, A., Mensah, A., Mohr, C., Nemitz, E., O'Dowd, C., Ovadnevaite, J., Pandis, S. N., Petaja, T., Poulain, L., Saarikoski, S., Sellegri, K., Swietlicki, E., Tiitta, P., Worsnop, D. R., Baltensperger, U., and Prevot, A. S. H.: Organic aerosol components derived from 25 AMS data sets across Europe using a consistent ME-2 based source apportionment approach, Atmos Chem Phys, 14, 6159-6176, DOI 10.5194/acp-14-6159-2014, 2014.

Reyes-Villegas, E., Green, D. C., Priestman, M., Canonaco, F., Coe, H., Prévôt, A. S. H., and Allan, J. D.: Organic aerosol source apportionment in London 2013 with ME-2: exploring the solution space with annual and seasonal analysis, Atmos. Chem. Phys., 16, 15545-15559, 10.5194/acp-16-15545-2016, 2016.

Sandradewi, J., Prévôt, A. S. H., Szidat, S., Perron, N., Alfarra, M. R., Lanz, V. A., Weingartner, E., and Baltensperger, U. R. S.: Using aerosol light abosrption measurements for the quantitative determination of wood burning and traffic emission contribution to particulate matter, Environmental Science and Technology, 42, 3316-3323, 10.1021/es702253m, 2008.

Weingartner, E., Saathoff, H., Schnaiter, M., Streit, N., Bitnar, B., and Baltensperger, U.: Absorption of light by soot particles: determination of the absorption coefficient by means of aethalometers, J Aerosol Sci, 34, 1445-1463, 10.1016/S0021-8502(03)00359-8, 2003.